Research Square

Preprints are preliminary reports that have not undergone peer review.
They should not be considered conclusive, used to inform clinical practice,
or referenced by the media as validated information.

Surface Passivation of Carbon Dots for Tunable Biological Performance

Mary M. Mikhail
Helwan University
Hanan B. Ahmed
Helwan University
Amira E. M. Abdallah
Helwan University
Mahmoud El-Shahat
National Research Centre
Hossam E. Emam
hossamelemam@yahoo.com

National Research Centre

Research Article

Keywords: Tunable CDs, Surface passivation, Optical characters, Tumor Anti-proliferative, Anti-inflammation.

Posted Date: March 13th, 2024

DOI: https://doi.org/10.21203/rs.3.rs-4021075/v1

License: This work is licensed under a Creative Commons Attribution 4.0 International License.
Read Full License

Additional Declarations: No competing interests reported.

Abstract

Recent investigations were shifted this trend toward exploring the biomedical applicability of CDs, relevant to chronic diseases. Herein, a systematic approach is demonstrated for studying tuning of optical character and biological performance for different surface passivated CDs. Alginate and pectin were successfully clustered oxygen-surface passivated CDs, while, chitin was used to nucleate nitrogen-surface passivated CDs. Pectin-treated with base (4.1 ± 1.8 nm) and chitin-treated acid (3.5 ± 1.7 nm) were ingrained the smallest O-surface passivated CDs and N-surface passivated CDs, respectively. However, N-surface passivated CDs were shown with the highest optical activity. CDs colloids prepared from alginate, pectin & chitin, resulted in reduction of tumor cell viability percentage to be 80.8%, 74.0% & 69.0% respectively. O-surface passivated CDs nucleated from alginate showed the highest anti-proliferative effects. Moreover, O-surface passivated CDs (from alginate) showed the supremacy in inhibition of inflammation, while, increasing of its concentration ten times resulted in significant increment in inhibition percent to be 28% & 42%, using 1 µg/mL & 10 µg/mL, respectively. So, O-surface passivated CDs (from alginate) can be applied as concurrent anti-inflammatory/antitumor drug, so as a potential therapeutic for treatment of inflammation, in production of vaccines, immune-therapeutics, and immune-suppressive drugs.

Introduction

Carbon Dots (CDs) were interestingly investigated as a new category of carbon-based nanomaterials [1], with particle size 1-10 nm, whereas, graphene nano-sheets exhibited with a plane size smaller than 100 nm were identified as graphene quantum dots (GQDs) [2]. CDs were firstly produced in 2004 within purifying single-walled carbon nanotubes [3]. Xu *et al.* are known as the first researchers who were firstly succeeded in the nucleation of CDs as a new family of nano-carbon based structures with superior optical performance [4, 5].

Consequently, the investigation of various synthesis techniques for clustering of CDs was an intensive researching purpose, attributing to their wide-scaled applications in extraordinary purposes such as in manufacturing of photovoltaic device, optoelectronic, bio-sensors, photocatalysts and drug delivery supporters [1-3, 6]. Compared to the conventional semiconducting quantum dots, CDs could be identified as biocompatible, chemically inert, non-toxic, with low cost, and exhibit superior optical performance [7]. CDs are known in terms of a surface-decorated carbonic core, whereas, CDs are quasi-circular carbon nanostructured objects, inbuilt of amorphous or nanocrystalline center with graphitic carbon (Sp^2 hybrid carbon) or mixed graphene and graphene-oxide sheets in a diamond-like Sp^3 hybridized carbons [1, 6, 7]. Simultaneously, CDs could be surface passivated with heteroatoms containing moieties, in order to enhance the degree of solubility in different aqueous solutions and to improve their potentiality for additional functionalization. So, by referring to the as-mentioned superior composition and characters, CDs are advantageous with tunable photoluminescence (PL), distinctive photo-induced electron transferring, capability for absorption of photovoltaic light, and infrared-responsive up-converted photoluminescence [1, 6, 7].

Sun et al, were firstly reported that CDs could be also identified as carbon nanosized photoluminescent structures [8], as they mentioned that; the recombination of excitons from the surface energy traps under irradiation that is affected with the surface passivation, reflects in the emission, and is known as the main reason for the superior optical character of CDs. Another research [9] identified CDs as a carbon core with a surface-decorating functional groups on the edge that composed from hybridizing the chemical groups, whereas, the decorated surface is known as photo-luminescent synergistic center of CDs. It was reported that, composition CDs with heteroatoms (such as O, N or S) in the main skeleton results in exhibition of CDs with tunable conduction/valence band position, with conferring unexpected function and application. Doping of nitrogen, metallic elements (e.g., Si, B, S, P, Mn, Mg, Cu, Zn, Tb, and Ru) within CDs matrix, was found to enhance the quantum yield of CDs, controlling the emission, for new functionality or applicability [10-13].

Nitrogen-based CDs were successfully nucleated from citric acid/urea and exhibited with blue and green emission via controlling the mass ratio of the nucleators [10, 12-15]. Interchanging the molar ratio of urea and sodium citrate from 3:1 to 6:1, 9:1, and 12:1, was shown to enhance the generation of CDs with emission bands at 450, 467, 536, and 526 nm, respectively [13]. Shamsipur et al. [11], were also succeeded in clustering of CDs (large in size) from amino acids as nitrogen containing nucleators. The composition of larger Sp^2 conjugation for carbons in the cores of the nucleated CDs leaded to emit at longer wavelength (yellow color). Whereas, the smallest sized CDs was observed with blue emission. Additionally, CDs with high nitrogen content could be successfully nucleated from aromatic amino acids to be exhibited with green emission [11].

Obeying green chemistry aspects, it is an interesting challenge to nucleate CDs that are exhibiting with both of anticancer and anti-inflammatory performance from biopolymers through the hydrothermal synthetic technique, to be applicable as anti-inflammatory and antitumor reagents. In recent decades, numerous reports were extensively considered with studying the biological performance and optical activities of carbon dots (CDs). Recent investigations were shifted this trend toward exploring the biomedical applicability of CDs, relevant to chronic diseases. Urgent requirement for medication from hazards human inflammation and cancer diseases are extensively considered, while, recent approaches were concerned with studying easily synthesized CDs as successfully effective therapeutics. Herein, a systematic approach is demonstrated for studying the tunability of optical character and biological performance for different surface passivated CDs, whereas, three different polysaccharides (alginate, pectin & chitin) were currently exploited as sprout for nucleation of differently surface passivated CDs under both of acidic and basic media and different temperature. Successive nucleation of CDs was affirmed via different instrumental analysis like, UV-Visible spectroscopy, TEM micrographs, XRD, FTIR, ^{1}HNMR& ^{13}CNMR spectral data. The optical properties of the synthesized CDs were investigated. The antitumor performance of CDs was evaluated via WST-1 Cell Proliferation Assay for analyzing their effects in the reduction cell viability percent for tumor cells. A comparable study for approving the anti-inflammatory action of the prepared CDs was presented, in order to show their supremacy for inhibition of inflammation.

Experimental section

Materials and chemicals

Chitin (Poly-(1→4)-β-N-acetyl-D-glucosamine, from shrimp shells, Sigma-Aldrich), pectin (Poly-D-galacturonic acid methyl ester, from citrus peel, galacturonic acid ≥74.0%, Sigma-Aldrich), alginate (Sodium alginate from brown algae, Sigma-Aldrich), sodium hydroxide (NaOH, 99%) and hydrochloric acid (HCl, 37%, Sigma-Aldrich) were all used as received and the stock solutions were prepared form distilled water.

Synthesis of water-soluble CDs

10 g/L of biopolymer (chitin, pectin or alginate) were dissolved within 40 g/L of NaOH to be kept under magnetic stirring for 120 minutes at 90 ℃. Consequently, under hydrothermal conditions, complete nucleation of CDs is performed, whereas, the prepared colloids were separately transferred to vertical hydrothermal autoclave reactor to be kept in oven at 210 ℃ for 6 hours. Lastly, the reaction colloids with dark brown color were left for cooling at room temperature, to be dialyzed with distilled water for purification to obtain highly purified/monodispersed/pure CDs, ready for further analysis. **Table 1** represents the experimental conditions for the currently prepared samples.

Table 1: Description of the synthesized samples.

Sample	Polysaccharide	Concentration (g/L)	NaOH (g/L)	HCl (ml/L)	Temperature (°C)	Time (hr)	Color
A1	Sodium alginate	10	10	-	150	3	Faint brown
A2	Sodium alginate	10	10	-	150	6	Brown
A3	Sodium alginate	10	10	-	200	3	Faint brown
A4	Sodium alginate	10	10	-	200	6	Brown
A5	Sodium alginate	10	-	10	200	3	colorless
A6	Sodium alginate	10	-	10	200	6	Faint yellow
A7	Sodium alginate	10	-	10	150	6	colorless
C2	Chitin	10	10	-	150	6	Faint yellow
C7	Chitin	10	-	10	150	6	Colorless
P2	Pectin	10	10	-	150	6	Brown
P7	Pectin	10	-	10	150	6	Colorless

Characterization and Instrumental analysis

Absorption spectral maps were manifested at 250–750 nm using a spectrophotometer (Cary 100 UV-VIS, UV–Vis-NIR Systems, from Agilent). Topography and size average of the synthesized CDs were determined via anticipation of HRTEM (JEOL-JEM-1200, from Japan). Size average of CDs was evaluated via 4 pi analysis software (from USA) for 50 particles at least. Mean size and poly-dispersity of CDs were also estimated using Zetasizer instrument "via dynamic light scattering technique at 25 °C in insulated chamber" (Malvern Nano ZS, from Malvern Instruments Ltd – UK). Infrared spectral data were obtained using Jasco FT/IR 6100 spectrometer. Absorbance spectral data were collected at "500 – 4000 cm^{-1} using 15 points smoothing, 4 cm^{-1} resolution, 64 scanning times with scanning rate of 2 $mm.sec^{-1}$". ^{1}H-NMR and ^{13}C-NMR spectra were estimated at Jeol-Ex-300 NMR spectrometry (JEOL – Japan). Photoluminescence spectral results for the prepared CDs in ultraviolet-visible range were obtained via spectro-fluorometer (JASCO FP8300), whereas, the measurement was carried out at room temperature with excitation at 340 nm, while, emission was detected at room temperature. All of the prepared CDs were analyzed via powder X-ray diffraction using "X'Pert MPD diffractometer system from Philips, at room temperature", while, Diffraction bands were collected in a diffraction angle (2θ) range of 3.5–50° "using monochromator, Cu Kα X-radiation at 40 kV, 50 mA and λ = 1.5406 Å".

Cell Proliferation Assay and Anticancer potentiality

Cell proliferation assay is performed for following up the physiology and physical changing for cells that were exposed to extracellular stimulation [16]. Sulforhodamine B (SRB) assay is a colorimetric examination mainly relies on the photoluminescence sulforhodamine B dye that could chemically bonded to basic amino acids in the vial cell. SRB assay could be ascribed as a cost effectiveness, accurate and highly sensitive test. Via the colorimetric detection, the total mass of proteins could be estimated via counting the number of cells. In this study, SRB assay was carried out to approve the anticancer potentiality of the prepared CDs and to monitor the effect of surface passivation on their anti-tumor performance against lung cancer cell (A-549). A-549 cell line was given from Nawah Scientific Inc., (Mokatam, Cairo, Egypt). Cells were allowed to gro in DMEM medium supplemented with "100 mg/mL of streptomycin, 100 units/mL of penicillin and 10% of humidified/heat-inactivated fetal bovine serum and five percent of (v/v) CO_2 atmosphere at 37 °C". Aliquots of "100µL cell (5x10^3 cells) were suspended in 96-well plates for incubation up to one day". The tested cells were mixed with another aliquot of "100 µL medium containing the prepared CDs with different concentrations". After 3 days, the tested cells were treated with "150 µL of 10% trichloroacetic acid to be incubated at 4°C for 60 minutes". Trichloroacetic acid was subsequently removed, while, the examined cells were washed for five times with distilled water. Aliquot of "70 µL SRB solution (0.4% w/v) was added to transfer cells for another time of incubation in dark at ambient conditions for 10 minutes". Afterword, the cells were washed for three times with "1% CH_3COOH for air-drying overnight". Lastly, 150 µL of TRIS (10mM) was exploited for dissolving the complex of protein-bonded with SRB dye, for detection of Absorbance at "540 nm via BMGLABTECH®-FLUOstar Omega microplate reader, Ortenberg, Germany".

Anti-inflammation Action:

RAW264.7 cells, "Muose macrophages, ATCC® , was obtained from Nawah Scientific Inc – Mokatam, Cairo, Egypt" were allowed to grow in "Dulbecco's Modified Eagle's Medium, DMEM, Corning, USA" to be supplemented with 10% of "fetal bovine serum", 100 U/mL of "penicillin", 100 µg/mL of "streptomycin sulphate" and 2 mM of "L-glutamine" in humidified incubator with "5% of carbon dioxide". Preliminary, cells were washed with "buffered phosphate saline" using sterile, then the flasks were scrapped off "SPL, Spain". Aliquot of "RAW 264.7 cells, 0.5×10^6 cells/mL" were allowed to implant in "96-well microwell plates" for overnight. Consequently, "non-induced triplicate wells" were added in a medium with samples vehicle, "DMSO, 0.1% v/v". the inflammation inducer with "lipopolysaccharide (LPS) as 100 ng/mL" was added to inflammation group of triplicate wells with a complete culturing media, containing 0.1% v/v of dimethyl sulfoxide. Triplicate welled samples were treated with screen concentrations of 10 and100 µM of CDs solubilized in dimethyl sulfoxide (0.1%, by volume) for dilution in LPS. 0.25 mM of Indo (Indomethacin) was applied as a blank sample. After incubation for 24 hours, Griess assay [17] was performed for estimating of nitrous oxide "NO" percent. Equal contents of Griess drug and culture supernatants were allowed for mixing and consequential incubation at ambient conditions for 10 minutes to produce colored diazonium salt and for estimating the absorbance at 540 nm on "Tecan Sunrise™ microplate reader" (Austria). NO Inhibition % of CDs was estimated according to LPS-induced

inflammatory groups, with normalization for the cell viability estimated via "Alamar Blue™ reduction assay" [18]. Concentration that inhibits fifty percent of LPS-induced NO was statistically evaluated on "GraphPad Prism software via the curve fitting to a non-linear regression modeling".

Results and discussion

Mechanism for nucleation of Tunable CDs

Comparative overview between the compatibility of chitin versus alginate and pectin for nucleation of water-soluble CDs under hydrothermal conditions was currently studied. The mechanism of CDs' clustering from alkali solubilized biopolymers could be postulated as follows; all of the as-exploited polysaccharides as CDs nucleators, are supposed to be fragmented under the strong alkaline conditions to their monomers, whereas, under consequential hydrothermal treatment, furfural intermediate is produced [19, 20], that in turn is polymerized, aromatized and oxidized for controllable nucleation of aromatic/nitrogen-surface passivated CDs from chitin, while, aromatic/oxygen-surface passivated CDs are supposed to be clustered from both of alginate and pectin [21, 22]. Eventually, dialysis was performed for ultra-purification to produce mono-dispersed/ ultra-filtered CDs with regulated geometrical features [23].

Characterization of CDs

UV-Visible spectral mapping for all of chitin, alginate and pectin, before and after their exploitation in preparation of CDs were plotted in **Figure 1**. Photos for the prepared samples under different conditions were presented in **Figure 1d**, whereas, it could be depicted that, the visual observation for the prepared colloids after exposure to hydrothermal treatment to complete the successive clustering of CDs, and regardless to the type of the exploited polysaccharide, acid hydrolysis resulted in producing turbid colorless or white colored colloids, while, under basic conditions, the obtained colloids were exhibited with brownish color in case of both alginate and pectin and faint brown in case of chitin

Figures 1a, 1b & 1c show the spectra of alginate, pectin and chitin before and after it exploitation as CDs nucleator, respectively, whereas, one absorption band at 270 – 285 nm with long tail in visible region was observed in spectrum of CDs ingrained from alginate-treated with acid (A7) and CDs nucleated from pectin-treated with either acid or base (P2 & P7). The as-mentioned peak is referring to π - π* transition and electron radiation relaxation [24, 25]. This data is in agreement with literature [26], whereas, the optical spectra of the all-prepared CDs are mainly observable in the ultraviolet range.

Figure 2 represents TEM micrographs of CDs that were successively ingrained from alginate-treated with base (A2, **Fig.2a**) and with acid (A7, **Fig.2b**), chitin-treated with base (C2, **Fig.2c**) and with acid (C7, **Fig.2d**) & pectin-treated with base (P2, **Fig.2e**) and with acid (P7, **Fig.2f**). The plotted data show the geometry and topographical features of the synthesized CDs, with the estimated size distribution of all the examined samples. All of the examined micrographs strongly affirmed the affinity and accessibility for all of the currently selected polysaccharides as CDs nucleators, for successive clustering of size and topography

controllable CDs, in addition to affirm the vital role of pH for ingraining spherical/highly monodispersed CDs. From the estimated data of size distribution, it could be revealed that, the exploitation of pectin-treated with base (P2, mean size 4.1 ± 1.8 nm) and chitin-treated acid (C7, mean size 3.5 ± 1.7 nm) resulted in ingraining of the smallest sized CDs with size distribution of 1.0-8.0 nm. Whereas, using of alginate either treated with acid (A7, mean size 6.8 ± 2.7 nm) or base (A2, mean size 6.5 ± 2.9 nm), pectin-treated with acid (P7, mean size 7.1 ± 2.6 nm) or chitin-treated base (C2, mean size 5.1 ± 1.9 nm), leaded to production of slightly bigger sized particles.

Moreover, Zetasizer data further affirmed TEM observations for successive nucleation of sized CDs [27, 28]. Comparative study for the particle size estimations detected via DLS analyzer for all of CDs prepared under basic conditions (**Figure 3a**) and acidic conditions (**Figure 3b**). Whereas, the represented data signed for the more preferability of pectin-treated with based and chitin-treated with acid for nucleation of the smallest particles compared to the others, while the particle size of CDs ingrained from pectin-treated with base and chitin-treated with acid was 15.7 nm and 10.1 nm, respectively. whereas, the largest sized particles were obtained from alginate-treated with base (28.2 nm) and pectin-treated with acid (18.2 nm). These findings could be explained due to, alkali hydrolysis of pectin is reported to increase the functionality of pectin biopolymeric blocks, and also chitin is well-known to exhibit higher reactivity in acidic medium rather than in basic medium, to be more accessible for nucleation of the desirable dots [29, 30]. So it could be concluded that, the plotted data in **Figures 2 &3** approved the accessibility of both alkali hydrolyzed pectin and acid-hydrolyzed chitin in synthesis of water soluble CDs under hydrothermal conditions, however, pectin is more favorable for clustering highly dispersed/homogenous and smaller sized regulated dots.

Optical Characters

According to literature, the optical characters of CDs were approved to be mainly correlated to the surface passivation rather than their particle size [26]. Meanwhile, it was reported that, the optical characters of CDs is mainly dependent on to the decorative functional groups on the surface of carbon core [31]. Surface functionalization means, the nucleation of CDs with florescence centers that are built up with the synergetic hybridization of heteroatom-containing functional groups on the surface of carbon core [32]. Thus, the optical characters of the as-nucleated CDs are dependent on the surface decorative groups inborn from either chitin or alginate and pectin, with overlapping of π-π* transition and n-π* transition of CDs. Additionally, surface passivation mainly reflects in chemical shifting for absorption in a longer wavelength, to produce colorful CDs and endowing their easy colorimetric detection.

Therefore, the optical characters of the as-clustered CDs were studied via photoluminescence spectral maps (**Figure 4**), whereas, the emission spectral data was estimated after excitation at 450 nm (**Figure 4a**). The observable emission bands in UV-visible range affirmed the presence of mobile π electrons and non-bonding electrons on the plenty of aromatized carbon-based skeleton and heteroatoms. Regardless to the type of polysaccharide, photoluminescence spectral data of CDs that were currently prepared under either basic or acidic conditions approved their exhibition with optical characters.

Comparing between the plotted spectra in **Fig.4b & Fig.4c**, it could be revealed that, acid treatment of polysaccharides resulted in nucleation of CDs with quenching of photoluminescence, whereas, CDs clustered from base-hydrolyzed polysaccharides were observed with more intense emission bands. Meanwhile, **Figure 4b** shows that; the excited CDs ingrained under basic conditions were exhibited with PL emission peak at 475- 490 nm (bluish green region) [33-35]. Whereas, CDs ingrained from base-treated chitin (C2) showed with the highest intense band with blue shifting, while, the lowest intense emission band with red shifting was observed for CDs nucleated from base-hydrolyzed pectin. In summarization, PL results approved that, with hydrothermal technique, the exploitation of the currently applied polysaccharides under either acidic or basic conditions was succeeded in nucleation of CDs that could emit in visible region, i.e., with efficient fluorescent characters in visible range, that sequentially facilitate their application in biomedicine.

FT-IR, ^{1}HNMR & ^{13}CNMR

NMR spectral data were represented in **Figures 5 & 6** for elucidation of reaction mechanism and approval for successive nucleation of CDs from either chitin or pectin and alginate. Figure 5a, 5b & 5c show ^{1}HNMR for CDs prepared under basic conditions from alginate (A2), chitin (C2) and pectin (P2), respectively. **Fig.5a** shows that, CDs ingrained from pectin is characterized with significant peaks at 1.19-2.27 ppm, 3.81-3.99 ppm, 4.68-4.99 ppm, 5.91 ppm and 8.30-8.33 ppm, that are corresponding to protons of sp^3 C-H, protons attached to hydroxyl decorative groups, protons attached to carbonyl groups, protons of O-C-H alcohols, and protons of aromatic or sp^2 CH=CH protons, respectively. whereas, **Fig.5b** shows the characteristic peaks of CDs ingrained from chitin (C2) to detected at 1.82-2.004 ppm, 3.26-3.87 ppm, 4.56-5.08 ppm, 5.92-6.13 ppm, 7.25-7.57 ppm and 8.81-8.91 ppm, that are signing for protons of N-H (amine), protons of N-C-H (amine), protons attached to carbonyl groups, protons of N-H (amide), protons of C-H aromatic, C-H (aldehyde), respectively. Moreover, F **Fig.5c** that is represented for CDs clustered from pectin (P2) also shown with exhibiting the characteristic peaks of protons of sp^3 C-H, carbonyl alpha C-H, -O-C-H (alcohols), C-H alkene, C-H aromatic, and carboxylic O-H, that are detected at 1.08-1.81 ppm, 2.29-2.56 ppm, 4.56-4.80 ppm, 5.99-7.08 ppm, 8.003-8.32 and 8.87-9.64 ppm, respectively.

On the other hand, **Figure 6** represents ^{13}CNMR spectra of the above-examined CDs samples and it could be obviously observed that, the typical bands for CDs ingrained from alginate (A2) (**Fig.6a**) are detected at 16.99-23.51 ppm, 31.14-34.29 ppm, 57.53-61.36 ppm, 68.59-72.18 ppm, 167.91-171.27 ppm and 181.42-183.04 ppm, that are referring to carbons of CH_2 (sp^3), CH (sp^3), -C(sp^3), carbon attached to hydroxyl group, C=C aromatic or sp^2 carbons and carbons of C=O groups, respectively. **Fig.6b** shows the spectrum of CDs ingrained from chitin (C2) with corresponding peaks of carbons of CH_2 (sp^3), amine and amide without hydrogen, -C (sp^3), C-H aromatic, C-(aromatic without hydrogen) and CH (aldehyde), that are observed at 19.80-23.95 ppm, 58.25-58.63 ppm, 71.89 ppm, 135.96 ppm, 168.61-171.27 ppm and 178.43-181.64 ppm, respectively. Lastly, **Fig.6c** shows the spectrum of CDs ingrained from pectin, whereas, the significant bands of carbons of CH_2 (sp^3), CH (sp^3), -C(sp^3), O-C-H (alcohol), CH (aromatic)

and CH (aldehyde), are observably detected at 17.17-23.70 ppm, 31.30-37.60 ppm, 57.68-61.57 ppm, 68.77-72.47 ppm, 166.52-173.41 ppm and 180.16-183.10 ppm, respectively.

From the estimated data it could be decided that, in all of the examined samples of CDs, observation of characteristic peak of C-H aromatic, C-H (aldehyde), approved the elucidated mechanism of nucleating CDs via aromatization and oxidation of polysaccharides fragments under the currently designed conditions. Additionally, in case of C2, the estimation of significant peaks of protons of N-H (amine), protons of N-C-H (amine), protons attached to carbonyl groups and protons of N-H (amide), approved the affinity and compatibility of chitin as nucleator of N-surface passivated CDs, whereas, in case of A2 & P2, estimation of characteristic peaks of O-C-H alcohols and C-H aldehyde, revealed the suitability of both pectin and alginate in production of O-surface passivated CDs, as elucidated in the suggested mechanism.

Figure 7 represents FT-IR spectral results for all of the as-functionalized polysaccharides before and after their exploitation as nucleators of CDs, in order to show the effect of pH conditions on the chemical compositions and the surface passivation of the as-ingrained CDs. **Figure 7a** shows the characteristic peaks of native alginate, while, it was characterized with significant absorption peaks at 3278 cm^{-1}, 2888 cm^{-1}, 1574 cm^{-1}, 1388 cm^{-1} and 998 cm^{-1} were characteristic for O-H stretching, interlayer C-H (sp^3) stretch, C=O stretch, CH (Sp3) bend, and alkoxy C-O, respectively. However, after exploitation of alginate in nucleation of CDs, under basic conditions (A2) and acidic conditions (A7), it was observed that, for spectrum of A7, the characteristic bands of native alginate were retained but with weak intensity. However, spectrum of A2 is observed with the disappearance of the characteristic bands for interlayer C-H (sp^3) stretch & CH (sp^3) bend, while, the characteristic peaks of C=C stretch (aromatic) at 1558-1701 cm^{-1} and aromatic sp^2 CH bend at 864 cm^{-1} are observably detected, that are characteristic for aromatized CDs [36, 37]. **Figure 7b** represents the spectra of chitin before and after its application as CDs nucleator, under acidic conditions (C7) and basic conditions (C2). Pristine chitin is shown with significant bands pointed as follows; i) 3397 & 3237 cm^{-1}, corresponding to $-NH_2$ & O-H stretching vibration within intermolecular hydrogen bonding, ii) amide I (C=O) stretching and amide II (C-N) bending at 1606 and 1568 cm^{-1}, respectively, iii) bands of C=O in hydrogen bonding with N-H of the neighboring chain and C-O-C bending at 1540 and 939-1127 cm^{-1}, respectively [38]. whereas, from the plotted spectra it could be depicted that, the characteristic peaks of chitin, were all retained after exploiting of chitin as CDs nucleator under acidic conditions (C7). However, spectrum of C2 is observed with the disappearance of the characteristic bands for native chitin, while, a sharpened C=C stretch (aromatic) peak at 1554-1404 cm^{-1} and aromatic sp^2 CH bend peak at 864 cm^{-1}, were observably detected. Figure 7c, also shows that, similarly, CDs clustered via acid treatment of pectin (P7) was shown with the retained peaks of native pectin (3263 cm^{-1}, 2885 cm^{-1}, 1682-1586 cm^{-1}, 1338 cm^{-1} and 995 cm^{-1}, corresponding to O-H stretching, interlayer C-H (sp^3) stretch, C=O stretch, CH (Sp3) bend, and alkoxy C-O, respectively.), whereas, the spectrum of CDs ingrained from base-treated pectin was observed with the specialized bands of C=C stretch (aromatic) and aromatic sp^2 CH bend at 1562-1389 cm^{-1} and 849 cm^{-1}, respectively.

Figure 8 shows the obtained data of XRD analysis that were estimated for CDs ingrained from either chitin or alginate and pectin under basic conditions (**Fig.8a**) and acidic conditions (**Fig.8b**), to declare that, CDs that were ingrained from base-treated alginate were exhibited with six diffraction bands at 2θ= 28.5° (broad), 34.4°, 38.0° & 41.8° & 46.8° whereas, exploitation of acid-hydrolyzed alginate produced CDs that were exhibited with only three bands at 2θ= 31.8°, 45.6°, 56.7° & 75.5°. In case of CDs clustered from base-treated chitin were show with eight diffraction peaks at 2θ= 19.7°, 30.2°, 35.0°, 38.0° & 41.5° & 46.6°, while, using of acid-treated chitin as CDs nucleator reflected in production of CDs with two diffraction peaks at 2θ= 9.6° & 19.4°. Moreover, applying of base-dissolved pectin as CDs generator produced CDs with six diffraction bands 2θ= 24.5° (broad), 30.1°, 34.7°, 37.9° & 41.5°, whereas, acid hydrolysis of pectin, resulted in clustering of CDs with only three diffraction bands at 2θ= 23.5° (broad), 31.8°, 50.5° & 52.8°. These could reveal that, compared to acid-hydrolyzed polysaccharides, exploitation of base-hydrolyzed polysaccharides resulted in clustering of more crystalline/highly organized CDs.

CDs with Antitumor Performance via Necrosis

The affinity of any antitumor reagent for destroying alive tumor cells is known as cytotoxicity, while, such reagents were hypothesized to act in cell death via the induction of necrosis, or apoptosis (i.e., programmed cell death). According to literature [39], necrosis is considered as the most favorable mode of action for the anticancer drugs. Recent reports were interestingly considered for investigating the potentiality of various drugs that could act via the induction of apoptosis for the malignant cells. In more details, activating caspases is identified as the first essential step for induction and progression of necrosis. Caspases as endoproteases, are enzymes that mainly act in regulating necrosis signal network and inflammation, via staring of the cellular destruction, i.e., degradation of cyto-proteins or fragmentation of DNA [40]. According to literature [41], the antitumor performance and anti-proliferation of the prepared CDs in the current study could elucidated as follows; penetration of CDs via cell wall of the tested cancer cells causes the activation of caspases, as the as-synthesized CDs in cytoplasm of the tested cells could successively liberate ROS, that are reported to efficiently activate caspases, to act directly in necrosis.

Figure 9a represents the relationship between the estimated values of absorbance and the concentration of the synthesized CDs using base-treated polysaccharides, whereas, increment in the estimated value of absorbance, meaning that, more of viable cells. The plotted data obviously demonstrates that; regardless to the type of the exploited polysaccharide, the estimated value of absorbance was significantly lowered via increasing the concentration of the exploited CDs up to1000 µg/mL. **Figure 9b** shows the relationship between the concentration of CDs and the cell viability percent, as the antitumor performance of the tested CDs to follow the order of A2 > P2 > C2. Meanwhile, O-surface passivated CDs ingrained from base-treated alginate (A2) were shown with the highest necrotic effects against the tested tumor cells, while, N-surface passivated CDs were exhibited with the lowest anti-tumor action. Moreover, the cell viability percentage was significantly lowered from 23.1%, 18.1% & 17.6 % at using 100 m/L to 80.8%, 69.0% & 74.0% at using 1000 mg/L for CDs ingrained from alginate, chitin & pectin, respectively. So, it could be declared that; CDs ingrained from base-hydrolyzed alginate is shown with the highest anti-

proliferative action against the examined tumor cells. In summarization, the synthesized CDs from either chitin or alginate and pectin exhibited high stability and high cytotoxic effects against the examined cancer cells, and either N-surface functionalized CDs or O-surface functionalized CDs could be ascribed as superiorly bio-compatible tumor anti-proliferative candidates. Moreover, the data approved the seniority O-surface passivated CDs over N-surface passivated CDs to be exploitable as antitumor laborer.

Anti-inflammation performance of O-surface passivated CDs & N-surface passivated CDs

One of the consequential effects of inflammation is the decomposition of proteins [42]. Whereas, the denatured proteins contribute in extensive induction of the immune cells at the inflammation sites, resulting in dramatical transforming of the acute inflammation to chronic inflammation [42, 43]. In addition to, Tumorigenesis (the progress in the growth of tumor cells), is also known as a result of the chronic inflammation [44]. Transformation of the acute inflammation to chronic inflammation only takes a place when the mechanism that is responsible for controlling of the acute inflammation is inefficiently proceeded and the clearance of inflammation mediators is failed [45]. Consequently, the inflammation mediators continuously increase, resulting in the production of ROS (such as $O_2^{\cdot}$, $OH^{\cdot}$, $^1O_2$, and H_2O_2) and RNS 9nitrogen reactive species; such as $NO^{\cdot}$, $ONOO^-$) that mainly responsible for the deterioration of nucleic acids [45, 46]. Excessive amounts of ROS & RNS resulted in oxidation of biomolecular structures and deterioration of proteins and genes, resulting in progression of the acute inflammation to chronic inflammation [47]. So, it could be clarified that, the action of anti-inflammatory drugs in mainly maintained in speeding up the sweeping of ROS and RNS to inhibit the progress of inflammation process.

In the demonstrated work, Griess assay was performed for approving the affinity of the prepared tunable CDs as anti-inflammatory drugs, and for monitoring the effect of variation in surface passivation on the anti-inflammatory performance for N-surface passivated CDs versus O-surface passivated CDs. Herein, the nati-inflammation performance was monitored via following up the inhibition of nitrous oxide radicals ($NO^{\cdot}$) as one of RNS that mainly responsible for the transformation of acute inflammation to chronic inflammation. Via Griess assay, the higher is the anti-inflammation action, the higher is the inhibition % of $NO^{\cdot}$ (NO inhibition%). **Figure 9c** represents the relationship between the absorbance and the concentration of the synthesized CDs under basic conditions to declare that, regardless to the effect of surface passivation, increment of the concentration of CDs from 0.01 mg/L up to 10 mg/L, resulted in significant decrement of 50% for the detected absorbance values.

Figure 9d shows the effect of concentration for CDs prepared under basic conditions on NO inhibition%, while, the data clarified that, regardless to the variability in surface passivation, all of the prepared CDs were shown with efficient anti-inflammatory action. However, O-surface passivated CDs (ingrained from alginate) showed the supremacy in inhibition of inflammation, while, increasing of its concentration ten times resulted in significant increment in inhibition percent to be 26.7% & 40.8%, using 1 µg/mL & 10 µg/mL, respectively. So, it could be decided that; O-surface passivated CDs (clustered from alginate) exhibit high affinity to act as anti-inflammatory drug, so as to be exploited as a potential therapeutic for

treatment of inflammation, in production of vaccines, immune-therapeutics, and immune-suppressive drugs.

Mechanism of anti-inflammation actin of the prepared CDs could be briefly elucidated according to literature as follows; CDs can act as sweepers for ROS & RNS with delocalizing the electron density in their aromatic nuclei, so as they can decrease the oxidation stress of such RS to retard their effects in transforming the acute inflammation to chronic inflammation. Moreover, the currently prepared CDs with variable surface passivation functional could provoke low immune response [48].

Conclusion

In recent decades, numerous reports were extensively considered with studying the biological performance and optical activities of carbon dots (CDs). Recent investigations were shifted this trend toward exploring the biomedical applicability of CDs, relevant to chronic diseases. Urgent requirement for medication from hazards human inflammation and cancer diseases are extensively considered, while, recent approaches were concerned with studying easily synthesized CDs as successfully effective therapeutics. Herein, a systematic approach is demonstrated for studying tuning of optical character and biological performance for different surface passivated CDs, whereas, three different polysaccharides (alginate, pectin & chitin) were currently exploited as sprout for nucleation of differently surface passivated CDs under both of acidic and basic media and different temperature. Successive nucleation of CDs was affirmed via different instrumental analysis like, UV-Visible spectroscopy, TEM micrographs, XRD, FTIR, ^{1}HNMR& ^{13}CNMR spectral data. The optical properties of the synthesized CDs were investigated. The antitumor performance of CDs was evaluated via WST-1 Cell Proliferation Assay for analyzing their effects in the reduction cell viability percent for tumor cells. Under acidic conditions, N-surface passivated CDs, prepared from chitin, were exhibited with the smallest size distribution, whereas, largest sized O-surface passivated CDs nucleated from pectin. N-surface passivated CDs ingrained from chitin under basic conditions were shown with the highest optical activity. Moreover, CDs colloids prepared under basic conditions were shown to follow the trend of alginate > pectin > chitin, in the anticancer performance. Meanwhile, O-surface passivated CDs nucleated from alginate under basic conditions were shown with the highest anti-proliferative effects against the examined cancer cells. Similarly, under basic conditions, O-surface passivated CDs (ingrained from alginate) showed supremacy in inhibition of inflammation, while, increasing of its concentration ten times resulted in significant increment in inhibition percent. As a conclusion, N-surface passivated CDs exhibited with the highest optical character, while, O-surface passivated CDs ingrained from alginate showed the seniority over that nucleated from pectin in the antitumor and anti-inflammatory performance.

Declarations

AUTHOR INFORMATION

Corresponding Author

Hanan B. Ahmed, Chemistry Department, Faculty of Science, Helwan University, Ain-Helwan, Cairo 11795, Egypt, Email: hananbasiony@gmail.com

Hossam E. Emam, Department of Pretreatment and Finishing of Cellulosic based Textiles, Textile Research and Technology Institute, National Research Centre, Scopus affiliation ID 60014618, 33 EL Buhouth St., Dokki, Giza 12622, Egypt, Email: hossamelemam@yahoo.com .

Authors

Mary M. Mikhail: Chemistry Department, Faculty of Science, Helwan University, Ain-Helwan, Cairo 11795, Egypt.

Amira E.M. Abdallah: Chemistry Department, Faculty of Science, Helwan University, Ain-Helwan, Cairo 11795, Egypt.

Mahmoud El-Shahat: Photochemistry Department, Chemical Industries Research Institute, National Research Centre, 33 EL Buhouth St., Dokki, Giza 12622, Egypt.

Author contributions

All authors conceived of the presented idea. **Mary Mikhail as phD student,** carried out the experimental work. **Dr. Amira Abdallah and Dr. Mahmoud El-Shahat** followed up the experimental work, performed the analytic part and helped in data discussion. **Dr. Hossam Emam and Dr. Hanan Ahmed** figured out the data, discussed the results and presented the data. **Dr. Hanan Ahmed and Dr. Hossam Emam** supervised the findings of the work and wrote the manuscript.

Ethical approve

We confirm that all experimental protocol concerning anticancer and anti-inflammatory were carried out and approved by Nawah Scientific Inc – Mokatam, Cairo, Egypt.

We confirm that all methods were carried out in accordance with relevant guidelines and regulations.

We confirm that all methods are reported in accordance with ARRIVE guidelines.

Funding

There is no funding for this work.

Conflict of interest

The authors declare that they have no competing financial interest

Data availability

The all data generated or analyzed during the current study are included in this manuscript.

References

1. R. Wang, K.-Q. Lu, Z.-R. Tang, Y.-J. Xu, Recent progress in carbon quantum dots: synthesis, properties and applications in photocatalysis, Journal of Materials Chemistry A 5(8) (2017) 3717-3734.
2. Y. Dong, J. Lin, Y. Chen, F. Fu, Y. Chi, G. Chen, Graphene quantum dots, graphene oxide, carbon quantum dots and graphite nanocrystals in coals, Nanoscale 6(13) (2014) 7410-7415.
3. X. Xu, R. Ray, Y. Gu, H.J. Ploehn, L. Gearheart, K. Raker, W.A. Scrivens, Electrophoretic analysis and purification of fluorescent single-walled carbon nanotube fragments, Journal of the American Chemical Society 126(40) (2004) 12736-12737.
4. E.C. Oliveira, M.C.I.V. de Campos, A.S.A. Lopes, M.G.R. Vale, E.B. Caramão, Ion-exchange resins in the isolation of nitrogen compounds from petroleum residues, Journal of Chromatography A 1027(1-2) (2004) 171-177.
5. S.N. Baker, G.A. Baker, Luminescent carbon nanodots: emergent nanolights, Angewandte Chemie International Edition 49(38) (2010) 6726-6744.
6. Y. Wang, A. Hu, Carbon quantum dots: synthesis, properties and applications, Journal of Materials Chemistry C 2(34) (2014) 6921-6939.
7. S.Y. Lim, W. Shen, Z. Gao, Carbon quantum dots and their applications, Chemical Society Reviews 44(1) (2015) 362-381.
8. Y.-P. Sun, B. Zhou, Y. Lin, W. Wang, K.S. Fernando, P. Pathak, M.J. Meziani, B.A. Harruff, X. Wang, H. Wang, Quantum-sized carbon dots for bright and colorful photoluminescence, Journal of the American Chemical Society 128(24) (2006) 7756-7757.
9. S. Zhu, Y. Song, X. Zhao, J. Shao, J. Zhang, B. Yang, The photoluminescence mechanism in carbon dots (graphene quantum dots, carbon nanodots, and polymer dots): current state and future perspective, Nano research 8(2) (2015) 355-381.
10. X. Li, S. Zhang, S.A. Kulinich, Y. Liu, H. Zeng, Engineering surface states of carbon dots to achieve controllable luminescence for solid-luminescent composites and sensitive Be 2+ detection, Scientific reports 4 (2014) 4976.
11. M. Shamsipur, A. Barati, S. Karami, Long-wavelength, multicolor, and white-light emitting carbon-based dots: achievements made, challenges remaining, and applications, Carbon 124 (2017) 429-472.
12. M. Xu, G. He, Z. Li, F. He, F. Gao, Y. Su, L. Zhang, Z. Yang, Y. Zhang, A green heterogeneous synthesis of N-doped carbon dots and their photoluminescence applications in solid and aqueous states, Nanoscale 6(17) (2014) 10307-10315.
13. J. Zhou, Y. Yang, C.-y. Zhang, A low-temperature solid-phase method to synthesize highly fluorescent carbon nitride dots with tunable emission, Chemical communications 49(77) (2013) 8605-8607.
14. S. Qu, X. Liu, X. Guo, M. Chu, L. Zhang, D. Shen, Amplified spontaneous green emission and lasing emission from carbon nanoparticles, Advanced Functional Materials 24(18) (2014) 2689-2695.

15. X. Ren, X. Meng, J. Ren, F. Tang, Graphitic carbon nitride nanosheets with tunable optical properties and their superoxide dismutase mimetic ability, RSC advances 6(95) (2016) 92839-92844.
16. P. Skehan, R. Storeng, D. Scudiero, A. Monks, J. McMahon, D. Vistica, J.T. Warren, H. Bokesch, S. Kenney, M.R. Boyd, New colorimetric cytotoxicity assay for anticancer-drug screening, JNCI: Journal of the National Cancer Institute 82(13) (1990) 1107-1112.
17. M.-S. Yoo, J.-S. Shin, H.-E. Choi, Y.-W. Cho, M.-H. Bang, N.-I. Baek, K.-T. Lee, Fucosterol isolated from Undaria pinnatifida inhibits lipopolysaccharide-induced production of nitric oxide and pro-inflammatory cytokines via the inactivation of nuclear factor-κB and p38 mitogen-activated protein kinase in RAW264. 7 macrophages, Food chemistry 135(3) (2012) 967-975.
18. T. Oliveira, C.A. Figueiredo, C. Brito, A. Stavroullakis, A. Prakki, E. Da Silva Velozo, G. Nogueira-Filho, Effect of Allium cepa L. on lipopolysaccharide-stimulated osteoclast precursor cell viability, count, and morphology using 4', 6-diamidino-2-phenylindole-staining, International Journal of Cell Biology 2014 (2014).
19. J. Ryu, Y.-W. Suh, D.J. Suh, D.J. Ahn, Hydrothermal preparation of carbon microspheres from mono-saccharides and phenolic compounds, Carbon 48(7) (2010) 1990-1998.
20. W. Kwon, S. Do, S.-W. Rhee, Formation of highly luminescent nearly monodisperse carbon quantum dots via emulsion-templated carbonization of carbohydrates, RSC advances 2(30) (2012) 11223-11226.
21. T. Sakaki, M. Shibata, T. Miki, H. Hirosue, N. Hayashi, Reaction model of cellulose decomposition in near-critical water and fermentation of products, Bioresource Technology 58(2) (1996) 197-202.
22. B. Chen, F. Li, S. Li, W. Weng, H. Guo, T. Guo, X. Zhang, Y. Chen, T. Huang, X. Hong, Large scale synthesis of photoluminescent carbon nanodots and their application for bioimaging, Nanoscale 5(5) (2013) 1967-1971.
23. H. Li, H. Ming, Y. Liu, H. Yu, X. He, H. Huang, K. Pan, Z. Kang, S.-T. Lee, Fluorescent carbon nanoparticles: electrochemical synthesis and their pH sensitive photoluminescence properties, New Journal of Chemistry 35(11) (2011) 2666-2670.
24. Y.J. Kim, P. Guo, R.D. Schaller, Aqueous Carbon Quantum Dot-Embedded PC60-PC61BM Nanospheres for Ecological Fluorescent Printing: Contrasting Fluorescence Resonance Energy-Transfer Signals between Watermelon-like and Random Morphologies, The Journal of Physical Chemistry Letters 10(21) (2019) 6525-6535.
25. Z. Luo, Y. Lu, L.A. Somers, A.C. Johnson, High yield preparation of macroscopic graphene oxide membranes, Journal of the American Chemical Society 131(3) (2009) 898-899.
26. X. Gao, C. Du, Z. Zhuang, W. Chen, Carbon quantum dot-based nanoprobes for metal ion detection, Journal of Materials Chemistry C 4(29) (2016) 6927-6945.
27. H.B. Ahmed, H.E. Emam, Synergistic catalysis of monometallic (Ag, Au, Pd) and bimetallic (AgAu, AuPd) versus Trimetallic (Ag-Au-Pd) nanostructures effloresced via analogical techniques, Journal of Molecular Liquids 287 (2019) 110975.

28. H.E. Emam, Arabic gum as bio-synthesizer for Ag–Au bimetallic nanocomposite using seed-mediated growth technique and its biological efficacy, Journal of Polymers and the Environment 27(1) (2019) 210-223.
29. H.E. Emam, N.M. Saad, A.E. Abdallah, H.B. Ahmed, Acacia gum versus pectin in fabrication of catalytically active palladium nanoparticles for dye discoloration, International journal of biological macromolecules 156 (2020) 829-840.
30. H.B. Ahmed, N. Saad, H.E. Emam, Recyclable palladium based nano-catalytic laborer encaged within bio-granules for dye degradation, Surfaces and Interfaces 25 (2021) 101175.
31. Z.L. Wu, M.X. Gao, T.T. Wang, X.Y. Wan, L.L. Zheng, C.Z. Huang, A general quantitative pH sensor developed with dicyandiamide N-doped high quantum yield graphene quantum dots, Nanoscale 6(7) (2014) 3868-3874.
32. B. Zhang, C.y. Liu, Y. Liu, A novel one-step approach to synthesize fluorescent carbon nanoparticles, European Journal of Inorganic Chemistry 2010(28) (2010) 4411-4414.
33. S.P. Sasikala, L. Henry, G. Yesilbag Tonga, K. Huang, R. Das, B. Giroire, S. Marre, V.M. Rotello, A. Penicaud, P. Poulin, High yield synthesis of aspect ratio controlled graphenic materials from anthracite coal in supercritical fluids, ACS nano 10(5) (2016) 5293-5303.
34. M. Li, C. Yu, C. Hu, W. Yang, C. Zhao, S. Wang, M. Zhang, J. Zhao, X. Wang, J. Qiu, Solvothermal conversion of coal into nitrogen-doped carbon dots with singlet oxygen generation and high quantum yield, Chemical Engineering Journal 320 (2017) 570-575.
35. Y.T. Yew, A.H. Loo, Z. Sofer, K. Klímová, M. Pumera, Coke-derived graphene quantum dots as fluorescence nanoquencher in DNA detection, Applied Materials Today 7 (2017) 138-143.
36. L. Pereira, A.M. Amado, A.T. Critchley, F. Van de Velde, P.J. Ribeiro-Claro, Identification of selected seaweed polysaccharides (phycocolloids) by vibrational spectroscopy (FTIR-ATR and FT-Raman), Food Hydrocolloids 23(7) (2009) 1903-1909.
37. A. Pourjavadi, A. Harzandi, H. Hosseinzadeh, Modified carrageenan 3. Synthesis of a novel polysaccharide-based superabsorbent hydrogel via graft copolymerization of acrylic acid onto kappa-carrageenan in air, European Polymer Journal 40(7) (2004) 1363-1370.
38. J.P. Jadhav, S.S. Phugare, R.S. Dhanve, S.B. Jadhav, Rapid biodegradation and decolorization of Direct Orange 39 (Orange TGLL) by an isolated bacterium Pseudomonas aeruginosa strain BCH, Biodegradation 21(3) (2010) 453-463.
39. E. Arkan, A. Barati, M. Rahmanpanah, L. Hosseinzadeh, S. Moradi, M. Hajialyani, Green synthesis of carbon dots derived from walnut oil and an investigation of their cytotoxic and apoptogenic activities toward cancer cells, Advanced pharmaceutical bulletin 8(1) (2018) 149.
40. S. Elmore, Apoptosis: a review of programmed cell death, Toxicologic pathology 35(4) (2007) 495-516.
41. A. Milner, D. Palmer, E. Hodgkin, A. Eliopoulos, P. Knox, C. Poole, D. Kerr, L. Young, Induction of apoptosis by chemotherapeutic drugs: the role of FADD in activation of caspase-8 and synergy with death receptor ligands in ovarian carcinoma cells, Cell Death & Differentiation 9(3) (2002) 287-300.

42. C.M. Modi, P.R. Bhatt, K.B. Pandya, H.B. Patel, U.D. Patel, Comparative evaluation of in vitro anti-inflammatory activity of different extracts of selected medicinal plants from Saurashtra region, Gujarat, India, Int. J. Curr. Microbiol. Appl. Sci 8(5) (2019) 1686-1698.
43. S. Sakat, A.R. Juvekar, M.N. Gambhire, In vitro antioxidant and anti-inflammatory activity of methanol extract of Oxalis corniculata Linn, Int J Pharm Pharm Sci 2(1) (2010) 146-155.
44. M. Neagu, C. Constantin, C. Caruntu, C. Dumitru, M. Surcel, S. Zurac, Inflammation: A key process in skin tumorigenesis, Oncology Letters 17(5) (2019) 4068-4084.
45. H. Lu, W. Ouyang, C. Huang, Inflammation, a key event in cancer development, Molecular cancer research 4(4) (2006) 221-233.
46. W. Dröge, Free radicals in the physiological control of cell function, Physiological reviews (2002).
47. S. Chatterjee, T. Dziubla, D. Butterfield, Oxidative stress and biomaterials, Oxidative Stress and Biomaterials. doi 10 (2016).
48. M.A. Dobrovolskaia, S.E. McNeil, Immunological properties of engineered nanomaterials, Nature nanotechnology 2(8) (2007) 469-478.

Figures

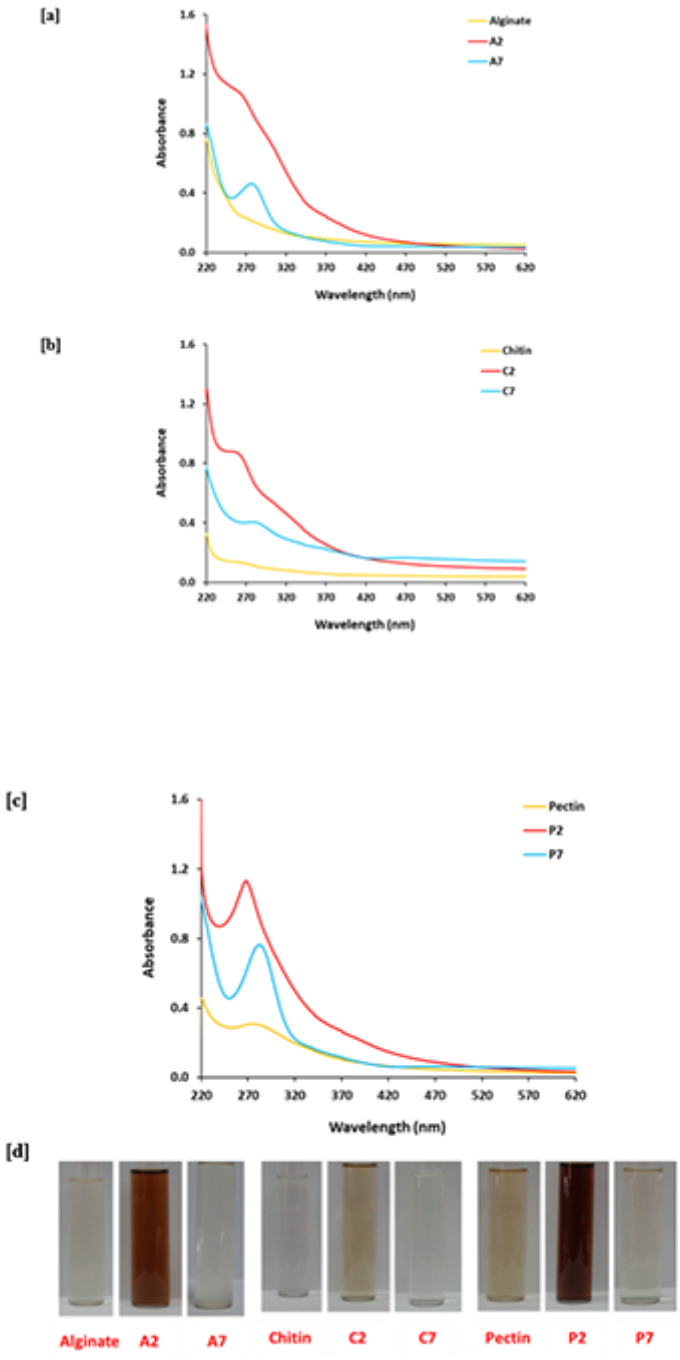


Figure 1

Absorbance spectra for the synthesized CDs samples; **[a]** A2, **[b]** A7, **[c]** C2, **[d]**C7, **[e]** P2 and **[f]** P7.

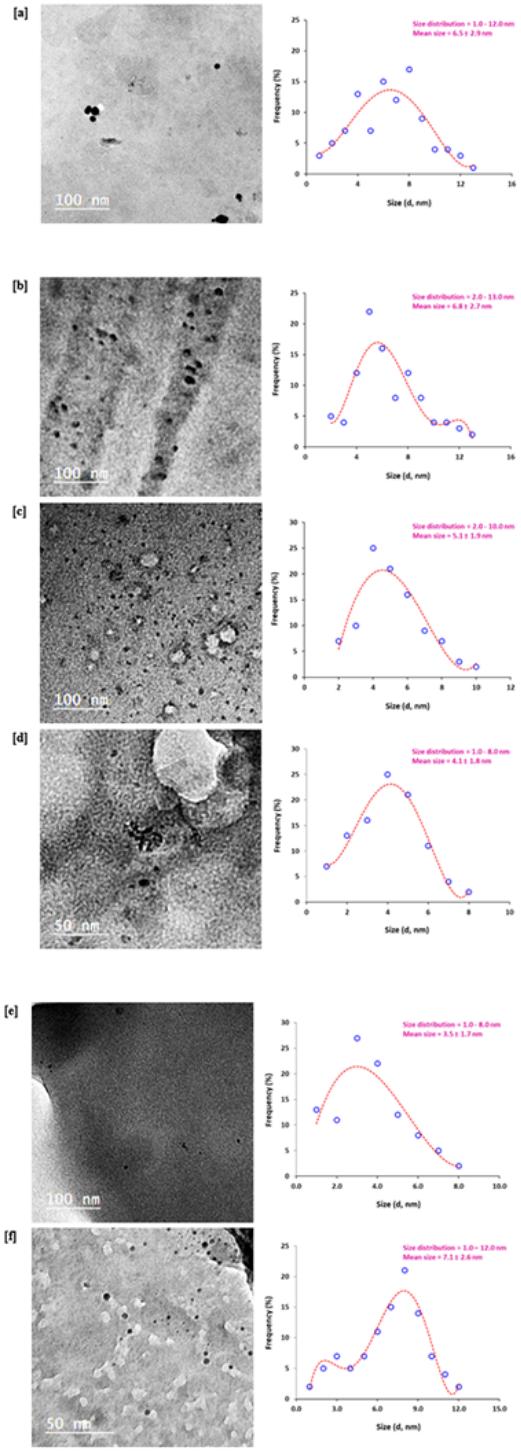


Figure 2

TEM and the calculated size distribution for the synthesized CDs samples; **[a]** A2, **[b]** C2, **[c]** P2, **[d]** A7, **[e]** C7 and **[f]** P7.

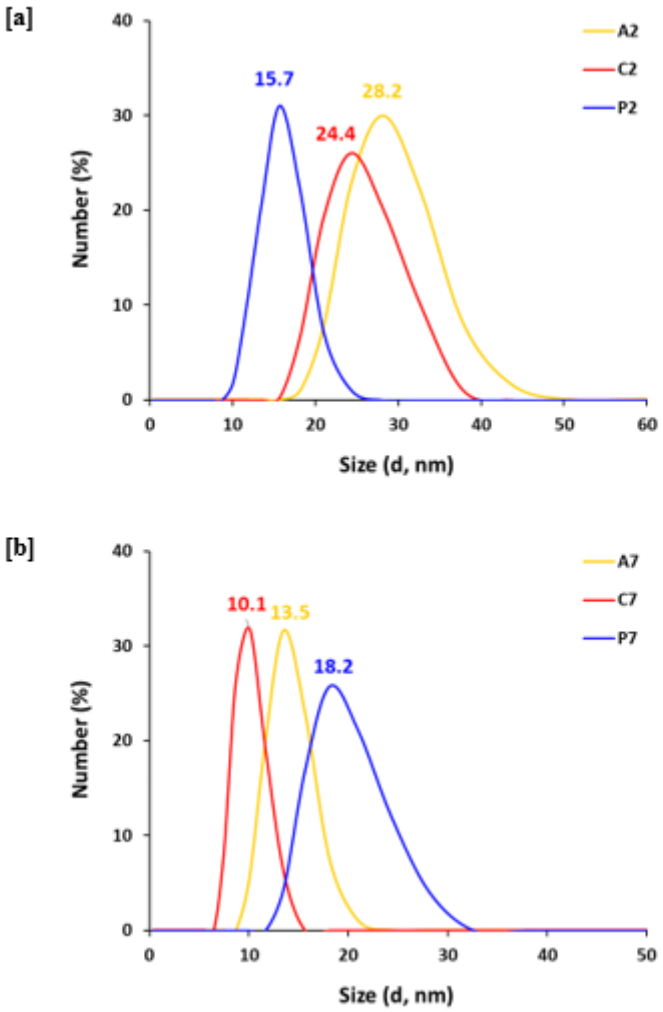


Figure 3

Particle size analyzer results for the synthesized CDs samples.

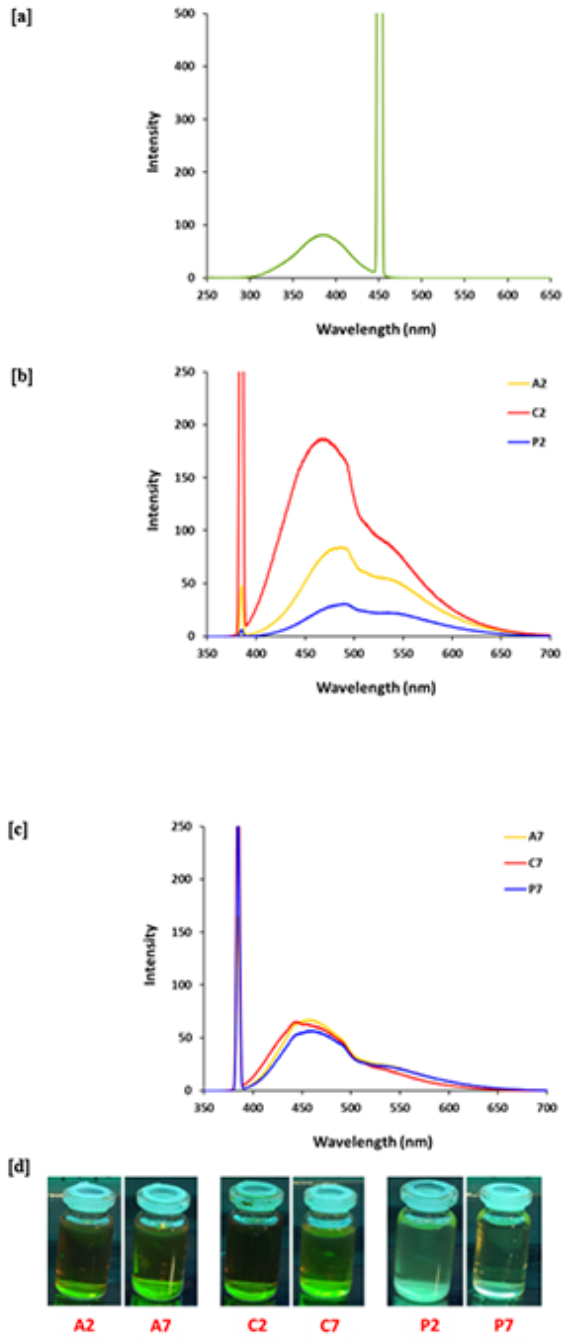


Figure 4

Fluorescence properties for the synthesized CDs samples; **[a]** excitation spectra for A2 (emission wavelength = 450 nm), **[b, c]** emission spectra (excitation wavelength = 380 nm) and **[d]** photographic images under UV-lamp (365 nm).

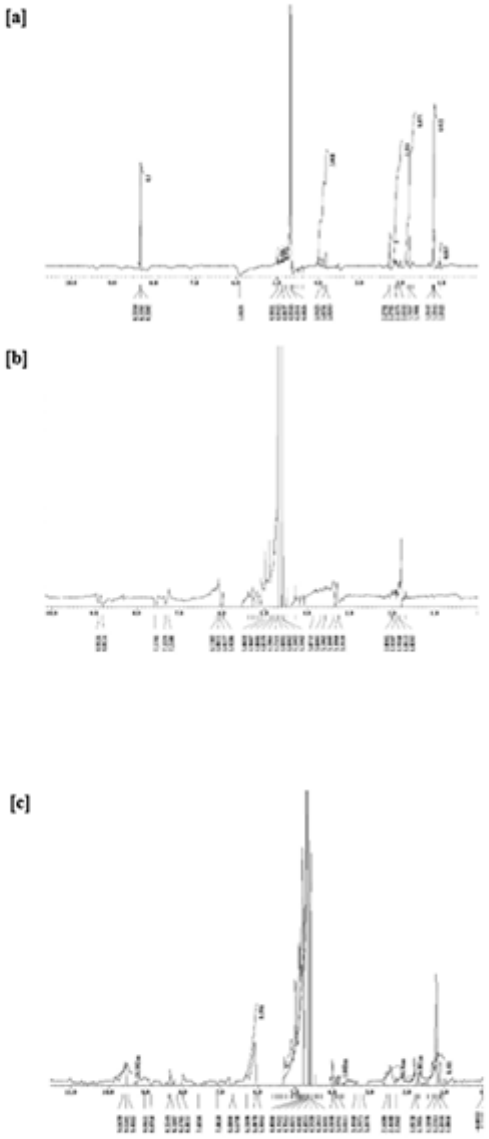


Figure 5

^{1}HNMR Spectral data for the synthesized CDs samples; **[a]** A2, **[b]** C2 and **[c]** P2.

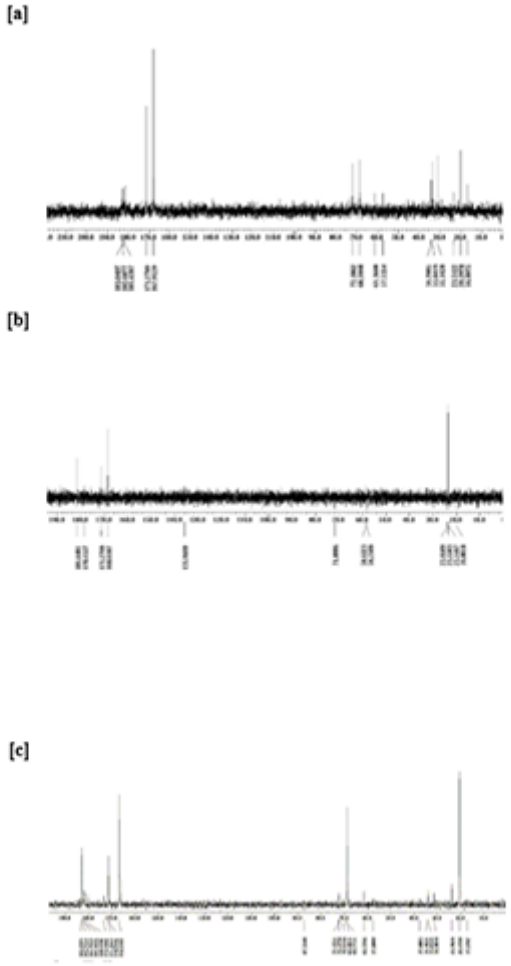


Figure 6

^{13}CNMR Spectral data for the synthesized CDs samples; **[a]** A2, **[b]** C2 and **[c]** P2.

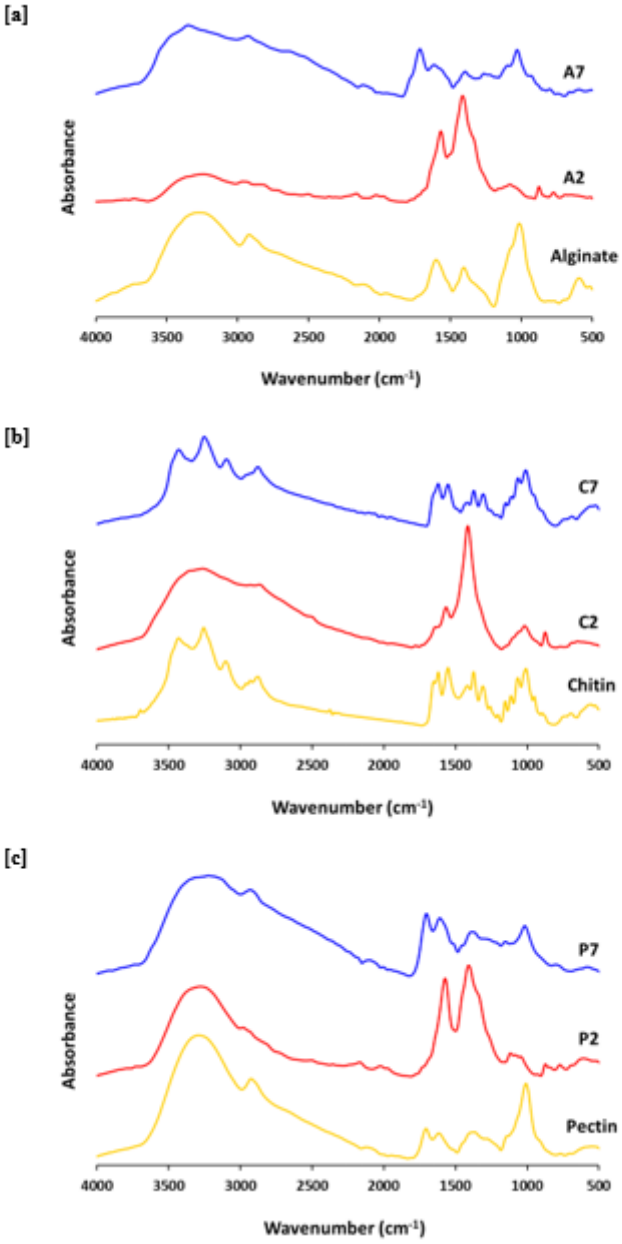


Figure 7

IR spectral data for the synthesized CDs samples.

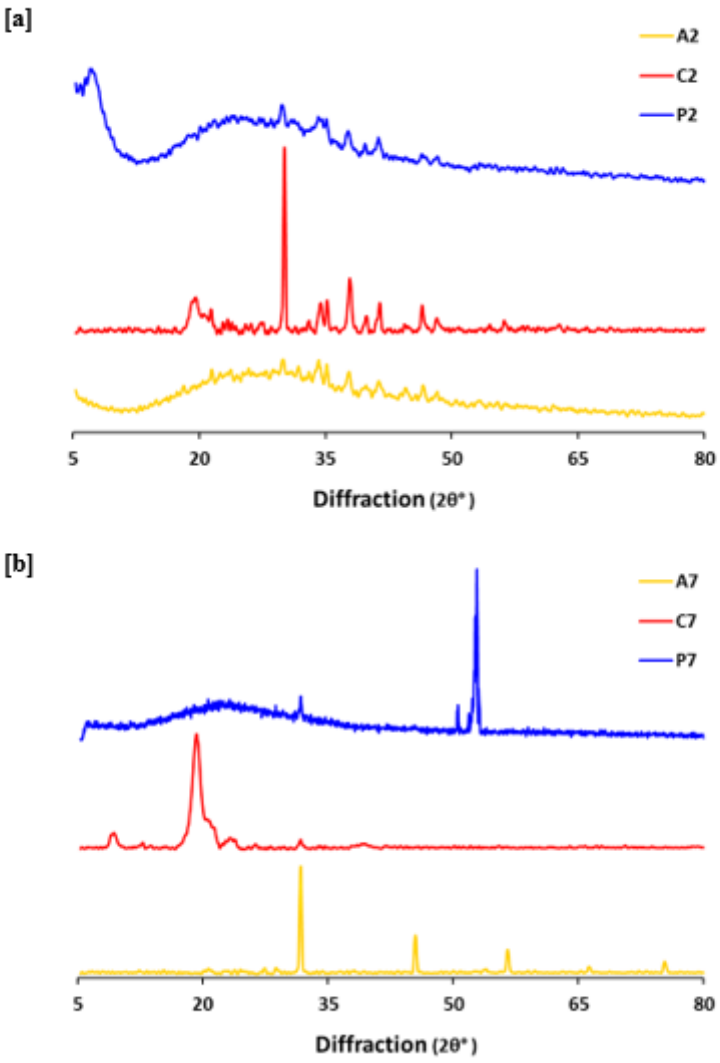


Figure 8

XRD results for the synthesized CDs samples.

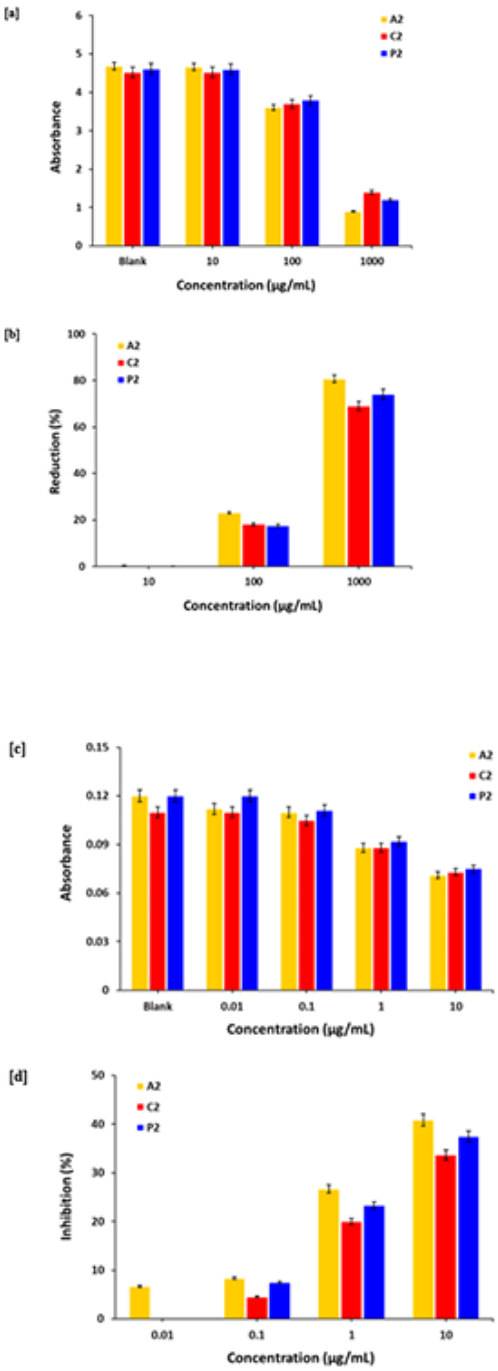


Figure 9

Biological activities for the synthesized CDs samples; **[a, b]** anti-cancer activity, **[c, d]**anti-inflammatory activity, **[a, c]** absorbance and **[b, d]**inhibition percentage.

Supplementary Files

This is a list of supplementary files associated with this preprint. Click to download.

- Supplementarydata.docx